NJC

Accepted Manuscript

This is an *Accepted Manuscript*, which has been through the Royal Society of Chemistry peer review process and has been accepted for publication.

Accepted Manuscripts are published online shortly after acceptance, before technical editing, formatting and proof reading. Using this free service, authors can make their results available to the community, in citable form, before we publish the edited article. We will replace this *Accepted Manuscript* with the edited and formatted *Advance Article* as soon as it is available.

You can find more information about *Accepted Manuscripts* in the Information for Authors.

Please note that technical editing may introduce minor changes to the text and/or graphics, which may alter content. The journal's standard Terms & Conditions and the Ethical guidelines still apply. In no event shall the Royal Society of Chemistry be held responsible for any errors or omissions in this *Accepted Manuscript* or any consequences arising from the use of any information it contains.

ROYAL SOCIETY OF CHEMISTRY

www.rsc.org/njc

Synthesis, Spectroscopic Characterization, X-ray structure and Electrochemistry of New Bis(1,2-Diaminocyclohexane)Gold(III) Chloride Compounds and their Anticancer Activities against PC3 and SGC7901Cancer Cell lines

Said S. Al-Jaroudi[a], M. Monim-ul-Mehboob[a], Muhammad Altaf[a], Mohammed Fettouhi[a], Mohammed I. M. Wazeer[a], Saleh Altuwaijri[b] and Anvarhusein A. Isab[a]*

[a]*Department of Chemistry, King Fahd University of Petroleum and Minerals, Dhahran 31261, Saudi Arabia.*

[b]*Clinical Research Laboratory, SAAD Research and Development Center, SAAD Specialist Hospital, Al-Khobar 31952, Saudi Arabia*

Abstract

New gold (III) compounds with chemical formulae [Au{*cis*-(1,2-DACH)}$_2$]Cl$_3$ **1**, [Au{*trans*-(±)-(1,2-DACH)}$_2$]Cl$_3$ **2** and [Au{(*S*,*S*)-(+)-1,2-(DACH)}$_2$]Cl$_3$ **3** (where 1,2-DACH = 1,2-Diaminocyclohexane) have been synthesized. The synthesized compounds were characterized using elemental analysis, various spectroscopic techniques including UV-Vis, FTIR spectroscopy, solution and solid-state NMR measurements; and X-ray crystallography. The stability of compounds **1**, **2** and **3** was checked by UV-Vis spectroscopy and NMR measurements. The electrochemical behavior was also investigated through cyclic voltammetry. The potential of the three compounds as anticancer agents was investigated by measuring *in vitro* cytotoxicity in terms of IC$_{50}$ and inhibitory effect on growth of human prostate (PC3) and gastric (SGC7901) cancer cell lines. [Au{(*trans*-(±)-(1,2-DACH)}$_2$]Cl$_3$ (**2**) showed better *in vitro* inhibitory effect on growth of human prostate (PC3) and gastric (SGC7901) cancer cell lines than [Au{(*cis*-(1,2-DACH)}$_2$]Cl$_3$ (**1**) and [Au{(*S,S)*-(+)-(1,2-DACH)}$_2$]Cl$_3$ (**3**).

Keywords: Bis-1,2-diaminocyclohexane gold(III) chloride compounds, 1,2-diaminocyclohexane, Crystal structure, Prostate cancer cells, Gastric cancer cells, Inhibitory effect on cell growth, *in vitro* Cytotoxicity

New Journal of Chemistry Accepted Manuscript

Author for correspondence: aisab@kfupm.edu.saTel : +966-13-860-2645

New Journal of Chemistry Accepted Manuscript

1. Introduction

To overcome drug resistance to early platinum drugs, the so-called third generation compounds were synthesized and one of the most promising drug is *oxaliplatin* [1-6], which bears a 1,2-diaminocyclohexane (DACH) ligand and an oxalate as a leaving group. The bulky chiral ligand, *R*,*R*-1,2-diaminocyclohexane (*R*,*R*-1,2-DACH), contributes to high cytotoxicity against *cis*platin-resistant cell lines, possibly due to the steric hindrance effect of the DACH-platinum-DNA adducts [7-10].

Gold (III) compounds, which are isoelectronic and isostructural to platinum(II) compounds, hold promise as possible anticancer agents [11-13]. Surprisingly, only a few reports exist in the literature describing the cytotoxic properties and the in vivo anticancer effects of gold (III) compounds [14-16]. Some preliminary data, suggesting a direct interaction with DNA as the basis for their cytotoxic effects, were previously reported [17-19]. Their mode of action is still unknown; however, several studies on cancer cell lines suggest they produce their antiproliferative effects through innovative and nonconventional modes of action [20-23]. Those having the same square-planar geometries as cisplatin [24], became the subject of increased anti-cancer research and hold great potential to enter clinical trials, since few of them are highly cytotoxic to solid cancer *in vitro* and *in vivo* while causing minimal systemic toxicity [25-29]. In general, gold (III) compounds are not very stable under physiological conditions due to their high reduction potential and fast hydrolysis rate. Therefore, selection of a suitable ligand to enhance the stability became a challenge in the design of gold(III) compounds as anticancer agents. The Au(III) ion is best coordinated by at least two chelating nitrogen donors which lower the reduction potential of metal center and thereby stabilize the compound [30-32].

New Journal of Chemistry Accepted Manuscript

Structurally, DACH ligand has two asymmetric carbon centers, thus, DACH can exist in three isomeric forms, which are the enantiomers (*R*,*R*-1,2-DACH) (*trans*-1,2-DACH), (*S*,*S*-1,2-DACH), (*trans*-1,2-DACH) and the diastereoisomer (*R*,*S*-1,2-DACH) (*cis*-1,2-DACH). Since DACH is chiral, the relevance of stereochemical issues has been addressed by a number of investigators [33], which affect the cytotoxicity of compound [34]. In spite of conflicting views [35-39], the consensus is that the (*R*,*R*) isomer is generally more active than the (*S,S*) isomer [40-41], although activity has also been demonstrated with the (*R*,*S*) isomer [42].

While significant efforts have been devoted to the study of anticancer activity of platinum-DACH complexes, gold-DACH complexes [43] have received relatively little attention, in spite of their rich biological chemistry. As a continuation of our interest in the synthesis of gold (III) complexes and to better understand the chemical and physical behavior of biologically relevant *bis*-(1,2-DACH) gold (III) complexes, the chiral isomers [Au{*cis*-(1,2-DACH)}$_2$]Cl$_3$ **1**, [Au{*trans*-(±)-(1,2-DACH)}$_2$]Cl$_3$ **2** and [Au{(*S*,*S*)-(+)-1,2-(DACH)}$_2$]Cl$_3$ **3**, have been synthesized and fully characterized by FTIR, NMR, Elemental Analysis and UV-Vis. Scheme 1 illustrates the structures of the ligands and scheme 2 shows the possible structures of the reported compounds **1**, **2** and **3**. Their cytotoxicity has been tested *in vitro* in human gastric cancer and cell line SGC7901 and prostate cancer cell lines PC3. In this study, the influence of relative stereochemistry of bis-(DACH) gold (III) complexes on their anticancer activity is addressed. In addition, it is found that these complexes are highly water soluble.

2. Experimental

2.1. Materials, chemicals and cell lines

New Journal of Chemistry Accepted Manuscript

$HAuCl_4 \cdot 3H_2O$ was obtained from Strem Chemicals Co. $NaAuCl_4 \cdot 2H_2O$ was purchased from Sigma-Aldrich. *cis*-1,2-diaminocyclohexane (*cis*-1,2-DACH), *trans*-(±)-diaminocyclohexane (*trans*-(±)-DACH) and (*S,S*)-(+)-diaminocyclohexane ((*S,S*)-(+)-1,2-DACH) were purchased from Aldrich. Absolute C_2H_5OH, D_2O and DMSO-d_6 were obtained from Fluka Chemicals Co. All other reagents as well as solvents were obtained from Aldrich Chemical Co., and used as received.

MTT (3-(4,5-Dimethylthiazol-2-yl)-2,5-diphenyltetrazolium bromide, a yellow tetrazole) was purchased from Sigma Chemical Co, St. Louis, MO, USA. Human gastric SGC7901 cancer and prostate PC3 cancer cell lines were provided by American Type Culture Collection (ATCC). Cells were cultured in Dulbecco's Modified Eagle Medium (DMEM) supplemented with 10 % fetal calf serum (FCS), penicillin (100 kU L^{-1}) and streptomycin (0.1 g L^{-1}) at 37 ºC in a 5 % CO_2 -95 % air atmosphere.

2.2 Mid and Far-FTIR measurements

The solid-state mid-FTIR spectra of free 1,2-diaminocyclohexane (1,2-DACH) ligands and their corresponding $[Au(1,2\text{-DACH})_2]Cl_3$ compounds were recorded on a Perkin-Elmer FTIR 180 spectrophotometer using KBr pellets over the range 4000-400 cm^{-1}. The CHN analyses of the compounds **1**, **2** and **3** are given in **Table 1** and the selected mid-FTIR frequencies are given in **Table 2**. Far-FTIR spectra were recorded for compounds **1**, **2** and **3** at 4 cm^{-1} resolution at room temperature. Cesium chloride (CsCl) disks were used on a Nicolet 6700 FT-IR with Far-IR beam splitter. The selected Far-IR data are presented in **Table 3**.

2.3. UV-Visible measurements

New Journal of Chemistry Accepted Manuscript

UV-Vis spectroscopy was used to determine the stability of the compounds in a physiological buffer (40 mM phosphate, 4 mM NaCl, pH 7.4). Electronic spectra were recorded on freshly prepared buffered solutions of each compound at room temperature. Then, their electronic spectra were monitored over 3 days at 37 ^{o}C. Electronic spectra were obtained for compounds **1**, **2** and **3** using Lambda 200, Perkin-Elmer UV-Vis spectrometer. The resulting UV-Vis absorption data are shown in **Table 4**.

2.4. Synthesis of Gold (III) compounds

Bis(1,2-diaminocyclohexane)gold(III) chloride compounds namely bis(*cis*-1,2-diaminocyclohexane)gold(III) chloride, [Au{*cis*-(1,2-DACH)}$_2$]Cl$_3$ **1;** bis(*trans*-(±)-1,2-diaminocyclohexane)gold(III) chloride, [Au{(*trans*-(±)-(1,2-DACH)}$_2$]Cl$_3$ **2**; and bis((*S,S*)-(+)-1,2-diaminocyclohexane)gold(III) chloride, [Au{(*S,S*)-(+)-(1,2-DACH)}$_2$]Cl$_3$ **3**; were synthesized by using two mole equivalent of *cis*-(1,2-DACH), (*trans*-(±)-(1,2-DACH) and (*S,S*)-(+)-(1,2-DACH) respectively with one mole equivalent of Chloroauric acid trihydrate $HAuCl_4 \cdot 3H_2O$ as described in literature for similar compounds [44]. Chloroauric acid trihydrate $HAuCl_4 \cdot 3H_2O$, 340 mg (1.0 mmol) was dissolved in 3 mL of water at ambient temperature. In a separate beaker, 1,2-diaminocyclohexane (1,2-DACH), 228 mg (2.0 mmol) was dissolved in in 2 mL of diethyl ether (DEE). Both solutions were mixed and a gummy yellow precipitate was formed. Upon adding 9 mL of aqueous ethanol solution (C_2H_5OH : H_2O = 7:1 v/v ratio) to the latter solution and followed by stirring the reaction mixture for about 1 h, a white precipitate of [Au(1,2-DACH)$_2$]Cl$_3$ was formed. The product was isolated and dissolved in 1 mL of water and recrystallized with addition of 5mL ethanol. The solid product was dried under vacuum. The yield of the compounds **1**, **2** and **3** was in the range of 65-70 %.

New Journal of Chemistry Accepted Manuscript

The compounds prepared in the present study were characterized by their CHN analysis, FT-IR and NMR spectroscopies and X-ray crystallography. The data of CHN analysis support the formation of the desired $[(1,2\text{-DACH})_2Au]Cl_3$ compounds **1**, **2** and **3**. Melting point (MP) / decomposition point (DP) and elemental analysis for compounds **1, 2** and **3** are presented in **Table 1**.

For compound **2**, $[Au\{(trans\text{-}(\pm)\text{-}(1,2\text{-DACH})\}_2]Cl_3$, all attempts were made in order to grow single crystals using different solvents and techniques but crystallization resulted in the resolution of the (*S,S*)-(+)-1,2-(DACH) based complex by formation of a co-crystal compound **2c** containing the bis-chelate $\{(S,S)\text{-}(+)\text{-}1,2\text{-DACH})\}_2Au(III)]Cl_3$ (**3**) and the mono chelate $[(S,S)\text{-}(+)\text{-}1,2\text{-}(DACH)AuCl_2]Cl$ [58]. The optimized crystal growth was observed in water over the span of two weeks. The X-ray structure of the co-crystal **2c** is reported here. The stability of compound **2** in aqueous solution was studied and confirmed by solution ^1H and ^{13}C NMR in D_2O. **Figure S1** shows the ^{13}C NMR spectra of: (a) compound **2**, $[\{trans\text{-}(\pm)\text{-}1,2\text{-DACH})\}_2Au(III)]Cl_3$, (b) compound **2c**, the co-crystal and (c) the mono chelate, $[trans\text{-}(\pm)\text{-}1,2\text{-}(DACH)AuCl_2]Cl$. The chemical shifts of C2 and C3 are lower in compound **2** compared with the mono chelate $[trans\text{-}(\pm)\text{-}1,2\text{-}(DACH)AuCl_2]Cl$. The values taken from the spectrum of the co-crystal **2c** are (64.46 and 32.82 ppm) and (65.68 and 33.15 ppm) respectively.

2.5. Solution ^1H and ^{13}C NMR measurements

All NMR measurements were carried out on a Jeol JNM-LA 500 NMR spectrometer at 298 K. The ^1H NMR spectra were recorded at a frequency of 500.00 MHz. The ^{13}C NMR spectra were obtained at a frequency of 125.65 MHz with ^1H broadband decoupling. The spectral conditions were: 32 k data points, 0.967 s acquisition time, 1.00 s pulse delay and 45 pulse angle. The

New Journal of Chemistry Accepted Manuscript

chemical shifts are referenced to 1,4-dioxane as an internal standard in ^{13}C NMR measurement. The ^{1}H and ^{13}C NMR chemical shifts are given in **Table 5** and **Table 6**, respectively.

2.6. Solid state ^{13}C NMR measurements

Solid-state ^{13}C NMR spectra were recorded at 100.613 on a Bruker 400 MHz spectrometer at ambient temperature of 298 K. Samples were packed into 4 mm zirconium oxide (ZrO) rotors. Cross polarization and high power decoupling were employed. Pulse delay of 7.0 s and a contact time of 5.0 ms were used in the CPMAS experiments. The magic angle spinning (MAS) rates were maintained at 4 and 8 kHz. Carbon chemical shifts were referenced to Tetramethylsilane (TMS) by setting the high frequency isotropic peak of solid adamantane to 38.56 ppm. The solid state NMR data are given in **Table 7**.

2.7. X-ray Diffraction

Quality single crystals for X-ray Diffraction were obtained from aqueous solutions and mounted in a thin-walled glass capillary on a Bruker-Axs Smart Apex diffractometer equipped with a graphite monochromatized Mo Kα radiation (λ = 0.71073 Å). The data were collected using SMART [45]. The data integration was performed using SAINT [46]. An empirical absorption correction was carried out using SADABS [47]. The structure was solved with the direct methods and refined by full matrix least square methods based on F^2, using the structure determination package SHELXTL [48] based on SHELX 97 [49]. Graphics were generated using ORTEP-3 [50] and MERCURY [51]. H atoms of DACH were placed a calculated positions using a riding model for both compounds **1** and **2c**. Both crystallize as hydrates from an aqueous solution, while the water H atoms in **1** were located on the Fourier difference map and

New Journal of Chemistry Accepted Manuscript

refined isotropically, those of complexes **2c** could not be located and therefore could not be placed at adequate positions. Crystal and structure refinement data are given in **Table 8**. Selected bond lengths and bond angles are given in **Table 9**.

2.8. Stability of Gold (III) complexes

Compounds **1, 2 and 3** were tested for their stability in water as well as mixed solvents of DMSO/water (2/1 v/v ratio) solution by ^{13}C and ^{1}H NMR. The compounds are highly soluble in water but sparingly soluble in DMSO [52]. To investigate the structural stability of the complexes, minimum of 30 mg/mL of representative gold (III) complexes **1, 2** and **3** were subjected to ^{1}H and ^{13}C NMR spectra analysis in DMSO-d_6/D_2O (v/v: 2/1, 1 mL). The duplicate samples were dissolved and immediately stored at room temperature and 37 ^{o}C, over time periods of 24 h and 72 h.

2.9. Electrochemistry

The electrochemical experiments were performed at room temperature using a potentiostat (SP-300, BioLogic Science Instruments) controlled by EC-Lab v10.34 software package. The electrochemical experiments were performed at room temperature. All the measurements were performed on solutions de-aerated by bubbling ultra-pure nitrogen for 15 min. The values of potential here reported were measured against a saturated calomel electrode (SCE). The cyclic voltammetry of the compounds **1, 2** and **3** were measured at scan rate of 50 mV/s on a reference buffer (40 mM phosphate, 4 mM NaCl, pH 7.4) using platinum as working electrode and graphite as a counter electrode with a concentration of 1.0 mM at room temperature. Ferrocene was used as pseudo reference to calibrate the working electrode. The couple $Fe^{III/II}$ formal

New Journal of Chemistry Accepted Manuscript

potential of ferrocene occur at $E^{\circ\prime}$ = +0.44 V (vs SCE) in 0.1M Bu_4NPF_6 solution in CH_3CN solvent which is similar to the report value under the same experimental condition [53]. Conversion to values vs ENH was obtained upon adding +0.24 V to the corresponding SCE values.

2.10. MTT assay for inhibitory effects of compounds (1–3) on PC3 and SCG7901 cancer cells

An MTT assay was used to obtain the number of living cells in the sample. Human gastric cancer SGC7901 and prostate cancer PC3 cells were seeded on 96-well plates at a predetermined optimal cell density, i.e. ca 6000 cells/100 μL per well in 96-well plates, to ensure exponential growth in the duration of the assay. After 24 h pre-incubation, the growth medium was replaced with the experimental medium containing the appropriate drug, using one of Bis(1,2-diaminocyclohexane)gold(III) chloride compounds **1**, **2** and **3** or a control using water. Six duplicate wells were set up for each sample, and cells untreated with drug served as a control. In one set of culture plates, human gastric cancer SGC7901 and human prostate PC3 cells were treated with 10 μM compounds **1**, **2** and **3** as the drug and the control (water) for 24, 48 and 72 h. In other sets, the compounds **1**, **2** and **3** with different concentration, i.e. 10, 20 and 30 μM, were employed to determine the growth inhibitory effect for both PC3 and SGC7901cells separately. After incubation, 10 μL MTT (6 g/L, Sigma) was added to each well and the incubation was continued for 4 h at 37 °C. After removal of the medium, MTT stabilization solution [dimethylsulfoxide (DMSO): C_2H_5OH = 1:1 in v/v ratio] was added to each well, and shaken for 10 min until all crystals were dissolved. Then, the optical density was detected in a micro plate reader at 550 nm wavelength using an Enzyme-Linked Immuno-Sorbent Assay (ELISA) reader.

New Journal of Chemistry Accepted Manuscript

After being treated with the compounds **1**, **2** and **3**, the cell viability was examined by MTT assay. Each assay was performed in triplicate. An MTT assay for the inhibitory effect has been used for compounds **1**, **2** and **3** against PC3 and SGC7901 cells. These cells were treated with various concentrations of compounds **1**, **2** and **3** for 24-72 h. The results are shown in **Figures 1** and **S2-S7**.

2.11. *in vitro* cytotoxic assay for PC3 and SGC7901 cancer cells

Human prostate PC3 and gastric SGC7901 cells were used in this study. Cells were cultured in Dulbecco's Modified Eagle Medium (DMEM) supplemented with 10 % fetal calf serum (FCS), penicillin (100 kU L^{-1}) and streptomycin (0.1 g L^{-1}) at 37 °C in a 5 % CO_2 - 95 % air atmosphere. Human gastric SGC7901 cells and prostate PC3 were incubated with these compounds at fixed concentrations or with water as a control to assess the inhibitory effect on cell growth. The standard MTT assay has been used to assess the inhibitory effect on cell growth. The cell survival versus drug concentration is plotted. Cytotoxicity was evaluated *in vitro* with reference to the IC_{50} value. The half maximal inhibitory concentration (IC_{50}) is a measure of the effectiveness of a compound to inhibit biological or biochemical functions. According to the FDA, IC_{50} represents the concentration of a drug/compound/complex that is required for 50% inhibition *in vitro*. It is evaluated from the survival curves as the concentration needed for a 50% reduction of survival. IC_{50} values are expressed in μM. The IC_{50} values were calculated from dose-response curves obtained in replicate experiments, as shown in **Table 10**.

3. Results and Discussion

3.1. Mid and Far-FTIR spectroscopic studies

New Journal of Chemistry Accepted Manuscript

The most significant bands recorded in the FTIR spectra of free ligand, mono- and bis-DACH compounds have been reported in **Tables 3** and **4**. It is noted that N-H stretching vibrations of compounds (**1-3)** are in the range 3333-3438 cm^{-1}, exhibiting blue shift compared with that of $-NH_2$ group of the corresponding free ligands. This is most likely due to stronger H-bonding interactions in the free ligands as compared to two coordinated amino- $:NH_2$ groups of 1,2-diaminocyclohexane (1,2-DAH) *via* donor N atoms, leading to formation of five member chelate with gold(III) center in corresponding compounds (**1-3**). The coordination of amino- $:NH_2$ with Au(III) center *via* nitrogen donor atom and formation of Au-N bond can be supported by the presence of ν(Au-N) at 419-428 cm^{-1}in Far-FTIR data [54]. The C-N stretching bands also showed a significant shift to higher wave number, indicating a shorter C-N bond in the compound than in the free ligand. Moreover, there was no signal observed at 352 and 367 cm^{-1} corresponding to the symmetric and asymmetric stretching of the Cl-Au-Cl bonds in $[(1,2\text{-DACH})AuCl_2]^+$ type compounds, indicating the absence of the mono-(1,2-DACH)gold(III) chloride compound [55]. The bis-(1,2-DACH)gold(III) chloride compounds **1-3** show N-H stretching frequencies generally lower in comparison with mono-(1,2-DACH)gold(III) chloride compounds (**Table 2**), most probably due to stronger hydrogen bonding interactions with the chloride anions in the bis-(1,2-DACH)gold(III) chloride compounds. Furthermore the Au-N stretching frequencies are consistent with weaker Au-N bond strength in compounds **1-3** compared to the corresponding mono-(1,2-DACH)gold(III) compounds (**Table 3**).

3.2. UV-Vis spectra

The λ_{max} values for the compounds studied along with their corresponding mono-(1,2-DACH)gold(III) chloride are shown in **Table 2**. The gold (III) compounds **1, 2** and **3** exhibit, in a reference buffered phosphate solution, intense transitions in the range 335-339 nm, which are

New Journal of Chemistry Accepted Manuscript

assigned to ligand-to-metal charge-transfer (LMCT) transitions characteristically associated with the gold (III) center [56]. These absorption bands were previously assigned as NH^- to gold (III) charge-transfer bands [56]. It is worth-mentioning that these spectral features appear only at relatively high pH values (pH > 6-7) at which ligand deprotonation has fully occurred. According to crystal field theory for d^8 compounds the lowest unoccupied molecular orbital (LUMO) orbital is d_{x2-y2}, so ligand to metal charge transfer (LMCT) could be due to $p_\sigma \rightarrow d_{x2-y2}$ transition [57]. It is a pertinent to mention that bis-(1,2-DACH)gold(III) chloride in comparison with their corresponding mono-(1,2-DACH)gold(III) chloride compounds [58] exhibit different λ_{max} values.

The electronic spectra of compounds **1, 2** and **3** were monitored at 37 ^oC over 3 days after mixing in the buffer solution. The spectra recorded just after mixing; and after 3 days are illustrated in **Figure 2**. It is apparently observed that the transitions remain relatively unmodified over a period of 3 days. Such observations show a substantial evidence for the stability of these compounds **1, 2** and **3** under the experimental conditions. Nevertheless, a slight decrease in intensity of the characteristic bands was noticed with time without significant modifications in shape of spectra. Further, such observation indicates that the gold center in these compounds remains in the +3 oxidation state. It is therefore expected that compounds **1, 2** and **3** would be stable enough in the physiological environment to undergo the necessary reactions/interactions required for bioactivity.

3.3. Solution NMR characterization

The ^1H and ^{13}C NMR chemical shifts of free ligand along with their corresponding compounds **1-3** are listed in **Tables 5** and **6**, respectively. In ^1H and ^{13}C NMR spectra of compounds **2** and

New Journal of Chemistry Accepted Manuscript

3, one quarter of the total expected number of signals is observed likely because of the D_2 symmetry. Whereas for compound **1,** ^{13}C NMR spectra show one half of the total expected number of carbon peaks. This is consistent with the solid state structure showing the molecule on an inversion center. The 1,2-diaminocyclohexane (1,2-DACH) ring is considered to be rigid hence allowing to distinguish equatorial H3 and H4 from axial H3 and H4 at room temperature. The proton signals of C-H connected to the amino ($-NH_2$) groups occur at 2.96-3.62 ppm as a multiplet, shifting downfield compared with the corresponding signals (2.23-2.25 ppm) in the free diamine ligands. The significant downfield shift was observed at 3.62 ppm for compound **1** with respect to the free DACH ligand at 2.23 ppm. This can be attributed to the donation of nitrogen lone pairs to the gold (III) center that causes de-shielding of the proton(s) next to the bonding nitrogen. ^{13}C NMR downfield shift was observed only for the carbon next to the bonding nitrogen. Conversely, the other carbons of the coordinated ligand (DACH) in the compound showed upfield shift. For instance, the chemical shifts of C3 and C4 for compound **1** are 26.46 and 20.80 ppm, respectively, whereas, those of the free 1,2-DACH ligand are 35.26 and 26.36 ppm. It is also worth-mentioning that compounds **1-3,** even though they have the same skeleton of 1,2-DACH, their carbon chemical shifts are different due to a different stereochemistry upon coordination.

3.4. Solid-state NMR characterization

At the spinning rate of 4 kHz, only the isotropic signals were observed for the carbons, indicating small anisotropy of the sp^3 hybridization of these atoms, except for compound **1** where a minor anisotropy was observed as shown in **Figure 3**. It also illustrates the four different peaks for the carbons connected to the amino ($-:NH_2$) group with equal intensity which supports the idea of the

New Journal of Chemistry Accepted Manuscript

inequivalence of the four carbon atoms, indicating that gold coordination sphere adopts a distorted square planar geometry.

Compared to solution chemical shifts, significant de-shielding in solid state is observed with similarity in chemical shift trends among all complexes **1-3** as given in **Table 7**, which is a clear indication of stability of the structural similarity in solid state as well as in solution.

3.5. X-ray crystal structure

The X-ray molecular structure of compound [Au{*cis*-1,2-DACH)}$_2$]Cl_3 **1** is shown in **Figure 4**. It corresponds to structure (a) in scheme 2. The asymmetric unit contains two Au(1,2-DACH) moieties with the gold (III) ions each located on a an inversion center. In both molecules, the metal ion is bonded to four nitrogen atoms of two *cis*-cyclohexane-1,2-diamine ligands in a distorted square planar geometry. The Au-N bond distances are in the range 2.031(2) - 2.038(2) Å and the N-Au-N chelate bond angles are 83.77(7)° and 83.22(7)° respectively for molecules **1** and **2** as given in **Table 9**. These values are similar to those reported for (cis-1,2-DACH)$AuCl_2$]Cl [58] and bis(ethylene-1,2-diamine)-gold(III) tris(perrhenate) [59]. The cyclohexyl rings adopt a chair conformation. The square planar geometry and the five-membered ring strain impose torsion angles N1-C1-C2-N2 of 51.31° and N3-C7-C12-N4 of 47.91° respectively for molecules **1** and **2**. Amine hydrogen atoms are engaged in hydrogen bonding interactions with Cl^- counter ions and the hydration water molecules generating a three-dimensional hydrogen bonding network as shown in **Figure S8**.

Compound **2c** crystallizes as a (1:1) co-crystal of the bis-chelate [Au{(*S,S*)-(1,2-DACH)}$_2$]Cl_3 **2** and the mono-chelate [(*S,S*)-(1,2-DACH)$AuCl_2$]Cl (**Figure 5**). The structure of the first component (molecule 1) of the co-crystal, namely [{(*S,S*)-(1,2-DACH)}$_2$Au]Cl_3, is distorted

New Journal of Chemistry Accepted Manuscript

square planar with the Au-N bond distances in the range 2.013(6) - 2.049(6) Å and the two N-Au-N chelate bond angles being 83.3(2) and 83.7(2)° respectively. These geometrical values are similar to those found for **1** and other bis-diamino-gold(III) compounds [59]. Similarly to compound **1**, the cyclohexyl rings adopt a chair conformation and the NH_2 groups have hydrogen bonding interactions with the chlorides and water molecules. The structure of the second component (molecule 2) of the co-crystal: [(*S,S*)-(+)-(DACH)$AuCl_2$]Cl, has been reported earlier by our group [58].

3.6. Stability Studies of Gold (III) compounds

NMR spectra of the compounds dissolved in D_2O and mixed DMSO-d_6/D_2O solvents (3:1 in v/v ratio) solution were obtained on immediate dissolution to serve as reference spectra and latter after 24 h (1 day) and after 72 h (3 days) in order to determine their stability at 37 ^oC in D_2O and at room temperature in mixed DMSO-d_6/D_2O. In general, all compounds **1**, **2** and **3** showed high stability in D_2O as well as in the mixed DMSO-d_6/D_2O as their NMR profiles remained unchanged over 3 days. For example, **Figures S9-S10** illustrate, respectively, ^1H and ^{13}C NMR profiles of the compound **1** at mixing and after 3 days in D_2O. Furthermore, the stability of compounds **1**, **2** and **3** in mixed DMSO-d_6/D_2O solvents was maintained and their NMR profiles remained unchanged even after 3 days under the same experimental conditions. **Figures S11-S12** show, respectively, ^1H and ^{13}C NMR profiles of compound **2** in DMSO-d_6/D_2O at mixing and after 3 days.

3.7. Electrochemistry of Gold (III) Compounds 1-3

New Journal of Chemistry Accepted Manuscript

The electrochemical behavior of compounds **1**, **2** and **3** along with their corresponding mono-(1,2-DACH)gold(III) compounds was investigated in a physiological environment through cyclic voltammetry to study the cyclohexanediamine bis-chelate effect on the stability of gold (III) compounds. The cyclic voltammetric curves of the compounds **1**, **2** and **3** and their corresponding (1,2-DACH)gold(III) compounds are shown in **Figure 6**.

Table 11 summarizes the cyclic voltammetric data for compounds **1**, **2** and **3**. The values of reduction potential vs. NHE exhibited by compounds **1**, **2** and **3** in a reference buffered phosphate, were in the range of (+465)-(+498) mV. Whereas, their corresponding mono-(1,2-DACH)gold (III) compounds showed reduction potential in the range of (+490)-(525) mV. In general, compounds **1**, **2** and **3** showed lower peak reduction potential values in comparison with their corresponding mono-(1,2-DACH)gold(III) compounds as presented in **Table 11**. This can be attributed to two fold chelate effect with reference to that of corresponding mono-(1,2-DACH)gold(III) compounds. In addition to this aspect the data also show that the *cis*-1,2-DACH complex is slightly more stable than the *trans*-(±)-(1,2-DACH) which is also consistent with the analysis of UV-Visible data. All compounds **1**, **2** and **3** show one irreversible reduction process which involves three electrons per mole in the controlled potential coulometry. The occurrence of Au(III)/Au(0) reduction is confirmed by the appearance of thin gold layer deposited on the platinum electrode surface after exhaustive electrolysis (*E*w, -0.7 V). In general, cyclic voltammetric results suggest that these compounds are quite stable under the physiological conditions.

New Journal of Chemistry Accepted Manuscript

3.8. Anti-cancer activity of Gold(III) compounds against PC3 and SGC7901 cancer cell lines

The MTT assay for time dependent inhibitory effect was performed with fixed concentration of compounds **1**, **2** and **3** on PC3 and SGC7901 cells for 24 h (1day) and 72 h (3 day). As illustrated in **Figures S2-S4**, compound **2** and purely optical active isomer compound **3** exhibited potentially high anticancer activity against gastric cancer cells SGC7901 and prostate cancer cells PC3 after 24 and 72 h of treatment with 10 μM. Whereas, compound **1** showed substantial inhibition against PC3 and SGC7901 cell lines under the same assay experimental condition. **Figure 1** illustrates the anticancer activity of compound **1-3** against the two cell lines. From **Figures S4-S6**, it is also quite clear that gold (III) compounds under study showed concentration dependent *in vitro* on the growth of cancerous cells PC3 and SGC7901 after 24 h. The *in vitro* cytotoxicity of compounds **1-3** was evaluated in terms of their IC_{50} values (**Table 10)** against prostate cancer cell lines (PC3) and gastric carcinoma cell lines (SGC7901). The IC_{50} data for the Au(III) complexes **1-3** showed reasonable cytotoxicity in the 6–10 μM range for SGC7901 cells. For SGC7901 cells, complex **2** was recognized as being as effective cytotoxic agent as *cis*-platin, while compound **1** and **3** demonstrated about 1.3 to 1.4-fold lower potency. For PC3 cells line, compounds **1-3** showed almost 6–13-fold lower cytotoxicity as compared to cis-platin.

As shown in Table 10, complexes **1-3** revealed an interesting feature that SGC7901/PC3 cancer cells exhibit 7 to 8-fold intrinsic resistance relative to the cis-platin [60]. This suggests that the intrinsic factors regulating cellular sensitivity to cis-platin are different for PC3 and SGC7901 cells. The factors affecting the sensitivity of PC3 and SGC7901 cells are similar in compounds **1-3**. There is no doubt that the present study is helpful for further exploiting and defining the potential role of gold(III) complexes in the combat against prostate and gastric cancers. The

New Journal of Chemistry Accepted Manuscript

cytotoxicity results for compounds **1-3** revealed that Gold (III) complex [Au{(*trans*-(±)-(1,2-DACH)}$_2$]Cl_3 (**2**) has a higher cytotoxic effect in comparison with the complexes **1** and **3.**

4. Conclusion

Three new gold (III) compounds **1**, **2** and **3** with general chemical formula of [Au(1,2-DACH)$_2$]Cl_3 have been synthesized. The compounds were characterized using elemental analysis, UV-Visible, Mid and Far-FTIR spectroscopy and solution and solid-state NMR measurements. The X-ray structures demonstrate that gold (III) coordination sphere adopts a distorted square planar geometry. The cytotoxic assays show that the compound [Au{(*trans*-(±)-(1,2-DACH)}$_2$]Cl_3 (**2**) is a more promising candidate as an anti-cancer agent than the *cis* isomer compound **1** and *trans* isomer compound **3**.

Supplementary material

Supplementary crystallographic data of CCDC deposit number is 889510 for compound **1** and 925974 for **2c.** They can be obtained free of charge *via* www.ccdc.cam.ac.uk/data_request/cif, by e-mailing data_request@ccdc.cam.ac.uk, or by contacting the Cambridge Crystallographic Data Centre, 12 Union Road, Cambridge CB2 1EZ, UK; fax: +44(0)1223-336033.

Acknowledgement

The author(s) would like to acknowledge the support provided by King Abdulaziz City for Science and Technology (KACST) through the Science & Technology Unit at King Fahd

New Journal of Chemistry Accepted Manuscript

University of Petroleum & Minerals (KFUPM) for funding this work through project No. **11-MED1670-04** as part of the National Science, Technology and Innovation Plan and to the Deanship of Scientific Research (DSR) for the internal project **IN 121049**.

References

[1] L. Kelland, Nat. Rev. Cancer 7 (2007) 573−584.

[2] A.M. Thayer, Eng. News 88 (2010) 24-28.

[3] G. Sava, A. Bergamo, P.J. Dyson, Dalton Trans. 40 (2011) 9069-9075.

[4] S. Dhar, S.J. Lippard, Bioinorganic Medicinal Chemistry, Wiley-VCH, Ch 3 (2011) 79-96.

[5] X.Wang, X.Z. Guo, Bioinorganic Medicinal Chemistry, Wiley-VCH, Ch 4 (2011) 97-149.

[6] J. Graham, M. Mushin, P. Kirkpatrick, Nat. Rev. Drug Discovery 3(2004) 11-12.

[7] J.L. Misset, H. Bleiberg, W. Sutherland, M. Bekradda, E. Cvitkovic, Crit. Rev. Oncol. Hematol. 35 (2000) 75-93.

[8] A.M. Di Francesco, A. Ruggiero, R. Riccardi, Cell. Mol. Life Sci. 59 (2002) 1914-1927.

[9] E.Raymond,S. Faivre, J.M.Woynarowski,S.G.Chaney,Semin.Oncol.25 (1998) 4-12.

[10] Z.Z. Zdraveski, J.A. Mello, C.K. Farinelli, J.M. Essigmann, M.G. Marinus, J. Biol. Chem. 277 (2002) 1255-1260.

[11] S. M. Janković, A. Djeković, Ž. D. Bugarčić, S. V. Janković, G. Lukić, M. Folic and D. Čanović, Biometals, 25 (2012) 919-925.

[12] O. Pinato, C. Musetti, N. P. Farrell, C. Sissi, J. Inorg. Biochem., 122 (2013) 23-37.

[13] G. V. Kalayda, C. H. Wagner, U. Jaehde, J. Inorg. Biochem., 116 (2012) 1-10.

New Journal of Chemistry Accepted Manuscript

[14] R.G.Buckley,A.M.Elsome,S.P.Fricker,G.R.Henderson,B.R.C.Theobald,R.V.Parish,B.P. Howe,L.R.Kelland, J. Med. Chem. 39 (1996) 5208-5214.

[15] P.Calamai,S.Carotti,A.Guerri,T.Mazzei,L.Messori,E.Mini,P.Orioli,G. P.Speroni,Anticancer Drug Des. 13 (1998) 67-80.

[16] F.Cossu,Z.Matovic,D.Radanovic,G.Ponticelli, Farmaco, 49 (1994) 301-302.

[17] V. Arsenijević, M. Volarević, M. Milovanović and Ž. D. Bugarčić, *Encyclopedia of Metalloproteins*, 2 (2013) 922-927.

[18] C. K.Mirabelli, R. K.Johnson,C. M.Sung,L. F.Faucette,K.Muirhead,S. T.Crooke, Cancer Res. 45 (1985) 32-39.

[19] S. T.Crooke,C. K.Mirabelli, Am. J. Med. 75 (1983) 109-113.

[20] R.W.Y. Sun, C.M. Che, Coord. Chem. Rev. 253 (2009) 1682–1691.

[21] Y. Wang, Q.Y. He, R.W.Y. Sun, C.M. Che, J.F. Chiu, Cancer Res. 65 (2005) 11553–11564

[22] K.H.M. Chow, R.W.Y. Sun, J.B.B. Lam, C.K.L. Li, A.M. Xu, D.L. Ma, R. Abagyan, Y. Wang, C.M. Che, Cancer Res. 70 (2010) 329–337.

[23] V. Petrović, M.Čolović, D. Krstić, A. Vujačić, S. Petrović, G. Joksić, Ž. Bugarčić, V. Vasić, J. Inorg. Biochem. 124 (2013) 35–41.

[24] L.Ronconi, C.Marzano, P.Zanello, M.Corsini, G.Miolo, C.Macca, A.Trevisan, D.Fregona, J Med Chem. 49 (2006) 1648-1657.

[25] L. Cattaruzza, D. Fregona, M. Mongiat, M. Ronconi, A. Fassina, A. Colombatti, D. Aldinucci, Int. J. Cancer 128 (2010) 206-215.

[26] L. Ronconi, D. Aldinucci, Q.P.D. Dou, Anticancer Agents Med Chem. 10 (2010) 283-292.

New Journal of Chemistry Accepted Manuscript

[27] V. Milacic, D. Chen, L. Ronconi, K.R. Landis-Piwowar, D. Fregona, Q.P. Dou, Cancer Res. 66 (2006) 10478-10486.

[28] Y.F. To, R.W.Y. Sun, V.S.F. Chen, W.Y. Chan, P.K.H. Yu, C.M. Tam, C. Che, L.S. Lin, Int. J. Cancer 124 (2009) 1971-1979.

[29] R.W.Y. Sun, C.M. Che, Coord. Chem. Rev. 253 (2009) 1682-1691.

[30] L.Giovagnini, L.Ronconi, D.Aldinucci, D.Lorenzon, S.Sitran, D.J.Fregoni. Med Chem 48 (2005)1588-1592.

[31] C.M.Che, R.W.Y.Sun, W.Y.Yu, C.B.Ko, N.Y.Zho, H.Z.Sun, ChemCommun, 8 (2003)1718-1729.

[32] A. Casina, C. Hartinger, C. Gabbiani, E. Mini, P.J. Dyson, B.K. Keppler, L. Messori, J InorgBiochem 102 (2008) 564-576.

[33] E.R.T.Tieking, Inflammopharmacology 16 (2008) 138-142.

[34] A.Casini, G.Kelter, C.Gabbiani, M.A. Cinellu, G. Minghetti, D. Fregona, H.H. Fiebig , L. Messori, J BiolInorgChem 14 (2009) 1139-1149

[35] M. Gulloti, A. Pasini, R. Ugo, S. Filippeschi, L. Marmonti, and F. Spreafico. Inorg.Chim.Acta. 91 (1984) 223-227.

[36] Y. Kidani, K. Inagaki, M. Iigo, A. Hoshi, and K. Kuretani. J. Med. Chem. 21 (1978) 1315-1318.

[37] M. Noji, K. Okamoto, Y. Kidani, and T. Tashiro. J. Med. Chem. 24 (1981) 508-515.

[38] Y. Kidani, M. Noji, T. Tashiro, Japanese Journal of Cancer Research (Gann), 71 (1980) 637-643.

[39] A. Pasini, A. Velcich, A. Mariani, Chem. Biol. Interact. 42 (1982) 311-320.

[40] J.H. Burchenal, K. Kalaher, T. O'Toole, J. Chisholm, Cancer Res. 37 (1977) 3455-3457.

New Journal of Chemistry Accepted Manuscript

[41] M.A. Bruck, R. Bau, M. Noji, K. Inagaki, and Y. Kidani, Inorg. Chim. Acta, 92 (1984) 279-284.

[42] J.F. Vollano, S. Al-Baker, J.C. Dabrowiak, J.E. Schurig, J. Med. Chem. 30 (1987) 716-719.

[43] M. Arsenijevic, M. Milovanovic, V. Volarevic, A. Djekovic, T. Kanjevac, A. Tatjana, D. Nebojsa, D. Svetlana, Z. Bugarcic, Med. Chem. 8 (2012) 2-8.

[44] B. P.Block, J. C.Bailar, J. Am. Chem. Soc. 73 (1951) 4722-4725.

[45] SMART APEX Software (5.05) for SMART APEX Detector, BrukerAxs Inc. Madison. Wisconsin, USA.

[46] SAINT Software (5.0) for SMART APEX Detector, BrukerAxsInc. Madison. Wisconsin, USA.

[47] G.M. Sheldrick, SADABS. Program for Empirical Absorption correction of Area detector Data. University of Gottingen, Germany, (1996).

[48] G.M. Sheldrick, SHELXTL V5.1 Software, Bruker AXS, Inc., Madison, Wisconsin, USA, (1997).

[49] G.M. Sheldrick, (1997), University of Gottingen, Germany.

[50] L.J. Farrugia, J. Appl. Cryst. 30 (1997) 565-565.

[51] C. F. Macrae, I. J. Bruno, J. A. Chisholm, P. R. Edgington, P. McCabe, E. Pidcock, L. Rodriguez-Monge, R. Taylor, J. van de Streek, P.A. Wood, J. Appl. Cryst. 41 (2008) 466-470.

[52] R. Ellson, R. Stearns, M. Mutz, C. Brown, B. Browning, D. Harris, S. Qureshi, J. Shieh, D. Wold, Comb Chem High Throughput Screen, 8 (2005) 489-98.

[53] J. Hans, A. Beckmann, H.-J. Kru¨ger, Eur. J. Inorg. Chem. (1999) 163-172

New Journal of Chemistry Accepted Manuscript

[54] K. Esumi, M. Nawa, N. Aihara, K. Usui, New J. Chem. 20 (1998) 719-720.

[55] I. Haruko, F. Junnosuke and S. Kazuo, Bull.Chem. Soc. Jpn. 40 (1967) 2584-2591.

[56] E. Kimura.; Y. Kurogi, T. Takahashi, *Inorg. Chem.* 30 (1991) 4117-4121.

[57] W. Beck, W.P. Fehlhammer, P. Pollmann, E. Schuierer, K. Feldl, Chem. Ber. 100 (1967) 2335-2361.

[58] S.S. Al-Jaroudi , M.Fettouhi, M.I.M. Wazeer, A.A. Isab, S.Altuwaijri, Polyhedron 50 (2013) 434-442.

[59] E. V. Makotchenko, I. A. Baidina. J. Struct. Chem., 52 (2011), 572-576.

[60] M. Monim-ul-Mehboob, M. Altaf, M. Fettouhi, A. A. Isab, M. I. M. Wazeer, M. N. Shaikh, S. Altuwaijri, Polyhedron 61 (2013) 225–234.

New Journal of Chemistry Accepted Manuscript

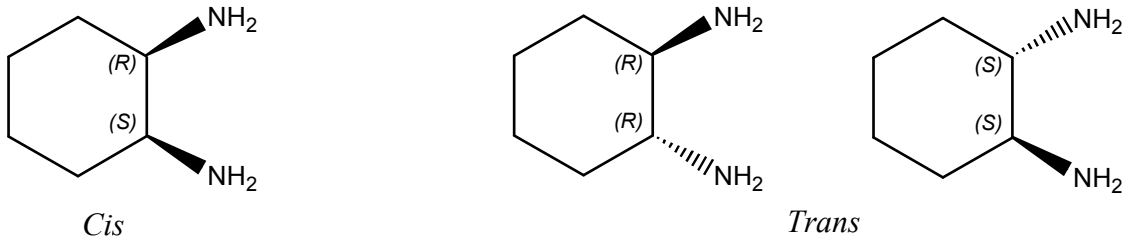

Scheme 1 Structures of *cis*- and *trans* isomers of 1,2-Diaminocyclohexane (1,2-DACH).

New Journal of Chemistry Accepted Manuscript

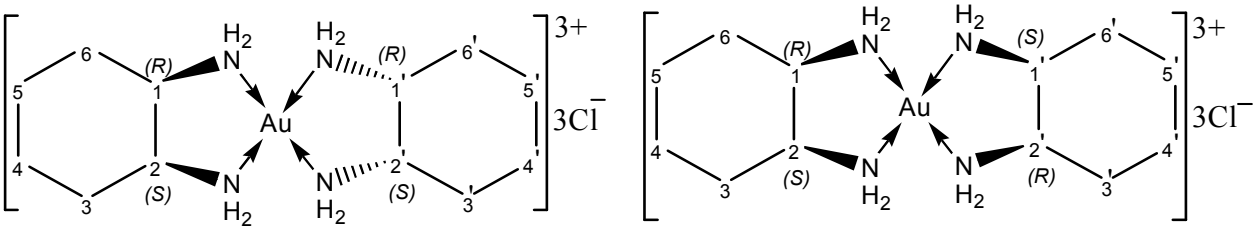

(a) (b)

Compound **1**, $[Au\{cis\text{-}(1,2\text{-DACH})\}_2]^{3+}$

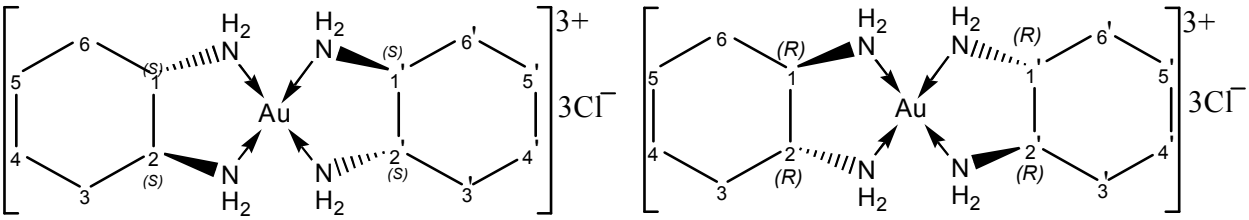

(a) (b)

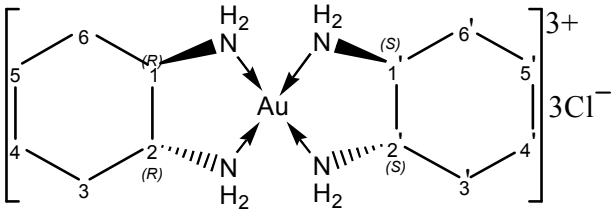

(c)

Compound **2**, $[Au\{trans\text{-}(\pm)\text{-}(1,2\text{-DACH})\}_2]^{3+}$

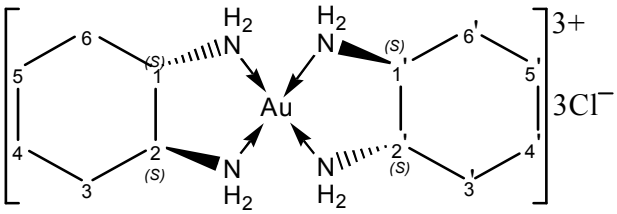

Compound **3**, $[Au\{(S,S)\text{-}(+)\text{-}(1,2\text{-DACH})\}_2]^{3+}$

Scheme 2 Possible structures of compounds **1**, **2**, and **3.**

New Journal of Chemistry Accepted Manuscript

Table 1: Melting point (MP)/Decomposition point (DP) and CHN analysis of compounds **1**, **2** and **3**.

Compound	MP/DP (°C)	Found (Calculated) %		
		H	C	N
1	203 (MP)	5.28(5.31)	27.03(27.11)	10.61(10.54)
2	170 (DP)	5.23(5.31)	26.97(27.11)	10.62(10.54)
3	174 (DP)	5.25(5.31)	26.99(27.11)	10.65(10.54)

New Journal of Chemistry Accepted Manuscript

Table 2: Mid-FTIR frequencies, ν (cm^{-1}) for compounds **1**, **2** and **3.**

Compound	ν(N-H)	$\Delta\nu_{shift}$	ν(C-N)	$\Delta\nu_{shift}$	Ref.
cis-(1,2-DACH)	3356 m, 3286 m		1092 s		[58]
[Au{*cis*-(1,2-DACH)}Cl_2]Cl	3414 w	93	1183 s	91	[58]
1	3409 m, 3338 m	53, 52	1185 s	93	[a]
trans-(±)-(1,2-DACH)	3348 m, 3271 m, 3183 m		1082 m		[58]
[Au{*trans*-(±)-(1,2-DACH)}Cl_2]Cl	3485 w, 3420 w, 3384 w	137, 149, 201	1175 m	93	[58]
2	3416 m, 3364 m, 3333 m	68, 93, 150	1176 m	94	[a]
(*S,S*)-(+)-(1,2-DACH)	3340 m, 3252 m, 3167 m		1082 m		[58]
[Au{(*S,S*)(+)(1,2-DACH)}Cl_2]Cl	3604 m, 3340 m, 3306 m	364, 88, 139	1171 m	89	[58]
3	3438 m, 3410 m, 3368 m	98, 158, 201	1181 m	99	[a]

[a]this work.

Table 3: Far-FTIR frequencies, ν (cm^{-1}) for compounds **1**, **2** and **3.**

Compound	ν(Au-Cl)	ν(Au-N)	Ref.
$HAuCl_4 \cdot 3H_2O$	369	-	[a]
[Au{*cis*-(1,2-DACH)}Cl_2]Cl	352, 367	437	[58]
1	-	428	[a]
[Au{*trans*-(±)-(1,2-DACH)}Cl_2]Cl	353, 365	437	[58]
2	-	419	[a]
[Au{(*S,S*)(+)(1,2-DACH)}Cl_2]Cl	353, 366	395, 436	[58]
3	-	427	[a]

[a]this work

New Journal of Chemistry Accepted Manuscript

Table 4: λ_{max} values for Au(III) compounds **1, 2** and **3** obtained from UV-Vis spectra.

Compound	λ_{max} (nm)	Ref.
$HAuCl_4 \cdot 3H_2O$	320	a
[Au{*cis*-(1,2-DACH)}Cl_2]Cl	302.5	[58]
1	338	a
[Au{*trans*-(±)-(1,2-DACH)}Cl_2]Cl	301.6	[58]
2	339.5	a
[Au{(*S,S*)-(+)-(1,2-DACH)}Cl_2]Cl	301.5	[58]
3	339	a

[a]this work.

Table 5: ^{1}H NMR chemical shifts of free ligands and corresponding compounds **1, 2** and **3** in D_2O.

Compound	^{1}H (δ in ppm)					
	H1,H2,H1′,H2′	H3,H6,H3′,H6′ Equatorial	H3,H6,H3′,H6′ Axial	H4,H5,H4′,H5′ equatorial	H4,H5,H4′,H5′ axial	Ref.
cis-(1,2-DACH)	2.23, *m*	1.85, *m*	1.69, *m*	1.28, *m*	1.12, *m*	[58]
1	3.62, *m*	1.94,*m*	1.77, *m*	1.57, *m*	1.38, *m*	a
trans-(±)-(1,2-DACH)	2.25, *m*	1.85, *m*	1.68, *m*	1.28, *m*	1.11, *m*	[58]
2	2.97, *m*	2.05, *m*	1.48, *m*	1.39, *m*	1.03, *m*	a
(*S,S*)-(+)-(1,2-DACH)	2.24, *m*	1.85, *m*	1.69, *m*	1.28, *m*	1.11, *m*	[58]
3	2.96, *m*	2.03, *m*	1.47, *m*	1.47, *m*	1.03, *m*	a

[a]this work

New Journal of Chemistry Accepted Manuscript

Table 6: Solution state ^{13}C NMR chemical shifts of free ligands and corresponding compounds **1, 2** and **3** in D_2O.

Compound	^{13}C(δ in ppm)			
	C1,C2, C1́,C2́	C3,C6, C3́,C6́	C4,C5, C4́,C5́	Ref.
cis-(1,2-DACH)	58.2	35.26	26.36	58
1	61.87, 61.80	26.46, 26.24	20.8	a
trans-(±)-(1,2-DACH)	58.46	35.55	26.63	58
2	64.56	32.93	24.15	a
(*S,S*)-(+)-(1,2-DACH)	58.27	35.32	26.43	58
3	64.49	32.93	24.1	a

[a]this work

Table 7: Solid state ^{13}C NMR chemical shifts of free ligands and corresponding compounds **1, 2** and **3**

Compound	^{13}C (δ in ppm)			
	C1,C2, C1́,C2́	C3,C6, C3́,C6́	C4,C5, C4́,C5́	Ref.
[Au{*cis*-(1,2-DACH)}Cl_2]Cl	69.20, 65.35	30.98	27.02, 22.12	[58]
1	66.61, 65.45, 64.57, 63.79	30.09, 29.49, 28.46, 27.77	23.54, 22.62	a
[Au{*trans*-(±)-(1,2-DACH)}Cl_2]Cl	69.6	37.37	27.99	[58]
2	69.14	36.89	28.42	a
[Au{(*S,S*)(+)(1,2-DACH)}Cl_2]Cl	70.21	37.86	29.16	[58]
3	68.39, 66.74 , 66.61	36.41	28.66, 26.32	a

[a]this work

New Journal of Chemistry Accepted Manuscript

Table 8: Crystal and structure refinement data for compounds **1** and **2c**

Compound	**1**	**2c**
CCDC deposit no.	889510	925974
Empirical formula	$C_{12}H_{34}AuCl_3N_4O_3$	$C_{18}H_{46}Au_2Cl_6N_6O_2$
Formula weight	585.75	985.24
Crystal size/mm	0.42 × 0.35 × 0.25	0.29 × 0.26 × 0.20
Wavelength/Å	0.71073	0.71073
Temperature/K	297 (2)	296 (2)
Crystal symmetry	Triclinic	Monoclinic
Space group	P -1	P 2_1
Unit cell dimensions		
a/Å	7.5342 (3)	7.3996 (13)
b/Å	11.7086 (5)	20.650 (4)
c/Å	12.0149 (5)	10.5543 (19)
α/°	103.096 (1)	-
β/°	91.041 (1)	93.558 (3)
γ/°	104.119 (1)	-
Volume ($Å^3$)	998.11 (7)	1609.6 (5)
Z	2	2
Calc. density ($g.cm^{-3}$)	1.949	2.033
μ(Mo-Kα)/mm^{-1}	7.79	9.63
F(000)	576	944
θ Limits/°	1.8–28.3	1.9–28.3
Collected reflections	13644	21865
Unique reflections(R_{int})	4175(0.021)	7311(0.043)
Observed reflections [I > 2σ (I)]	4932	7964
Goodness-of-fit on F^2	1.05	1.01
R_1(F), [I > 2σ (I)]	0.016	0.029
wR_2 (F^2), [I > 2σ(I)]	0.042	0.072
Largest diff. Peak and hole (e $Å^{-3}$)	0.99, -1.10	2.01, -0.89

New Journal of Chemistry Accepted Manuscript

Table 9: Selected bond lengths (Å) and bond angles (°) for compounds **1** and **2c**

Bond Angles (°)		Bond Lengths (Å)	
Compound **1**			
Molecule 1			
N2—Au1—N2^{i}	180.00 (13)	Au1—N2	2.0314 (17)
N2—Au1—N1	83.77 (7)	Au1—N2^{i}	2.0314 (17)
N2^{i}—Au1—N1	96.23 (7)	Au1—N1	2.0375 (18)
N2—Au1—N1^{i}	96.23 (7)	Au1—N1^{i}	2.0375 (18)
N2^{i}—Au1—N1^{i}	83.77 (7)		
N1—Au1—N1^{i}	180.00 (13)		
Molecule 2			
N4—Au2—N4^{ii}	180.00 (14)	Au2—N3^{ii}	2.0346 (18)
N4—Au2—N3^{ii}	96.78 (7)	Au2—N3	2.0346 (18)
N4^{ii}—Au2—N3^{ii}	83.22 (7)	Au2—N4	2.0309 (18)
N4—Au2—N3	83.22 (7)	Au2—N4^{ii}	2.0309 (18)
N4^{ii}—Au2—N3	96.78 (7)		
N3^{ii}—Au2—N3	180.00 (9)		

New Journal of Chemistry Accepted Manuscript

Compound **2c**

Molecule 1			
N1—Au1—N2	84.80 (19)	Au1—N1	2.038 (4)
N1—Au1—Cl2	90.78 (14)	Au1—N2	2.040 (5)
N2—Au1—Cl2	175.57 (15)	Au1—Cl2	2.272 (2)
N1—Au1—Cl1	175.01 (14)	Au1—Cl1	2.2727 (17)
N2—Au1—Cl1	90.21 (15)		
Cl2—Au1—Cl1	94.21 (9)		
Molecule 2			
N5—Au2—N6	83.7 (2)	Au2—N4	2.034 (6)
N5—Au2—N4	95.5 (2)	Au2—N3	2.049 (6)
N6—Au2—N4	179.2 (3)	Au2—N5	2.013 (6)
N5—Au2—N3	178.8 (2)	Au2—N6	2.029 (5)
N6—Au2—N3	97.5 (2)		
N4—Au2—N3	83.3 (2)		

Symmetry codes: (i) $-x+1, -y+2, -z+1$; (ii) $-x, -y, -z$

New Journal of Chemistry Accepted Manuscript

Table 10 *in vitro* Cytotoxicity data of compounds **1, 2** and **3** for 72 h exposure on PC3 and SGC7901cancer cell lines

	IC_{50} (μM)			
Compound	PC3	SGC7901	Fold resistance SGC7901/PC3	Ref.
Cis-platin	1.1 ± 0.10	7.3 ± 0.50	6.64	[60]
1	13.1 ± 0.13	10.4 ± 0.21	0.79	a
2	6.5 ± 0.07	5.8 ± 0.11	0.89	a
3	9.9 ± 0.21	9.5 ± 0.05	0.96	a

[a]this work

Table 11 Peak Potential values (vs ENH) for reduction of compounds $[Au(1,2\text{-DACH})Cl_2]Cl$ and corresponding $[Au(1,2\text{-DACH})_2]Cl_3$ compounds **1**, **2** and **3**

Compound	**E_p(mV)**
$[Au\{cis\text{-}(1,2\text{-DACH})\}Cl_2]Cl$	490
1	465
$[Au\{trans\text{-}(\pm)\text{-}(1,2\text{-DACH})\}Cl_2]Cl$	525
2	495
$[Au\{(S,S)(+)(1,2\text{-DACH})\}Cl_2]Cl$	522
3	498

New Journal of Chemistry Accepted Manuscript

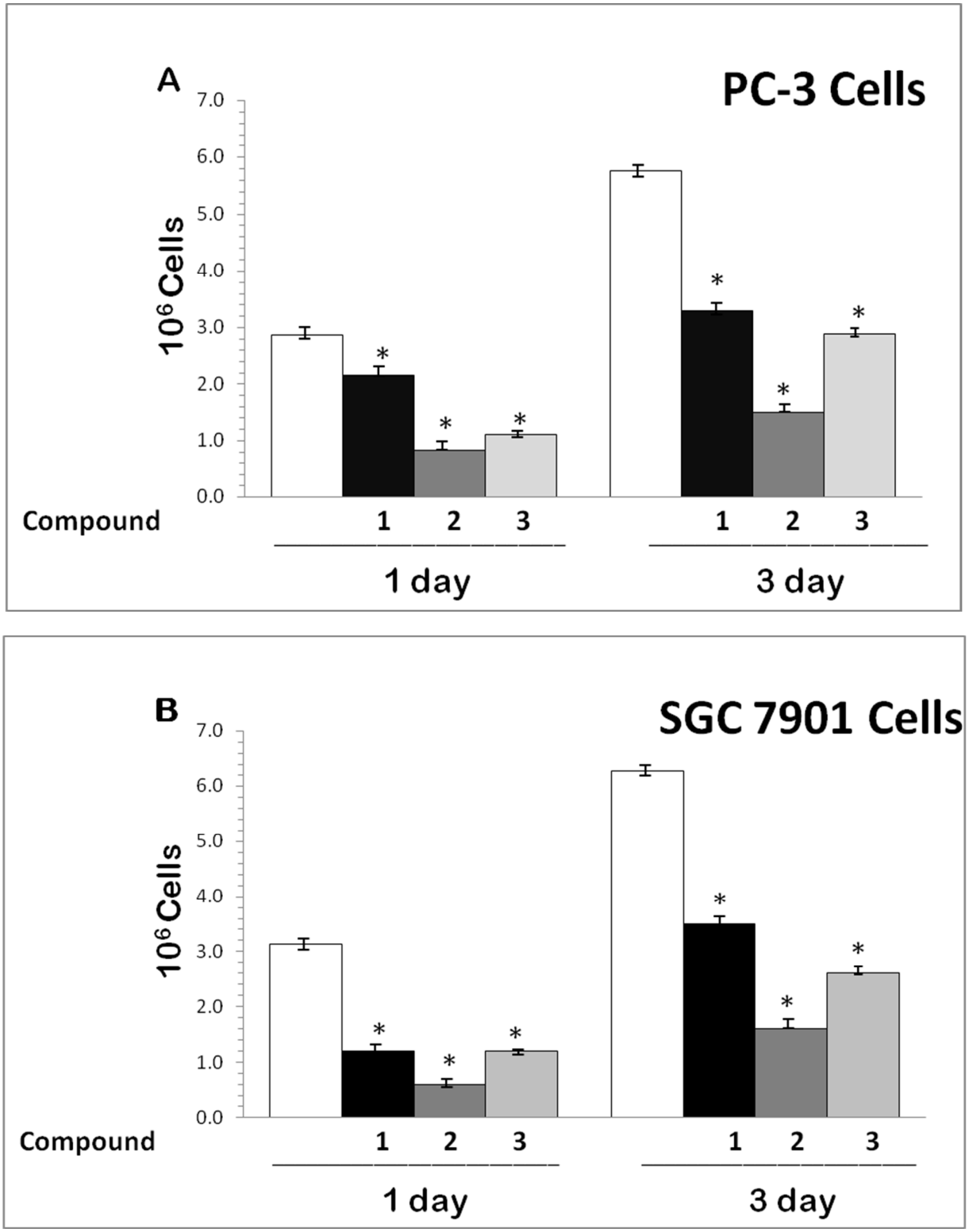

Figure 1 Comparative time dependent inhibitory effects for 10 μM of compounds **1**, **2** and **3** on growth of (A) PC3 and (B) SGC7901 cells for day 1, day 2 and day 3 using MTT. Results were expressed as the mean, SD. *P<0.05.

New Journal of Chemistry Accepted Manuscript

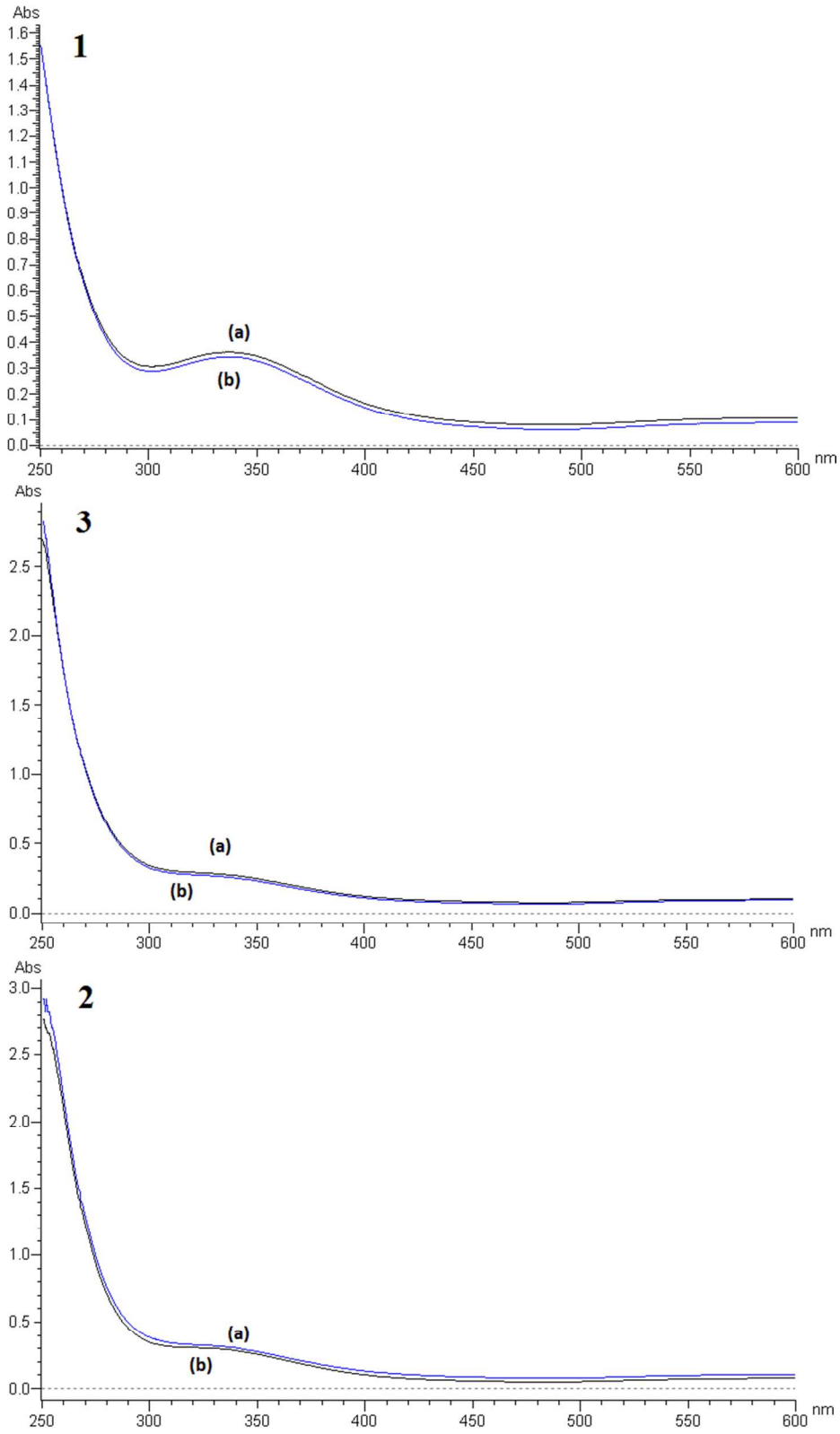

Figure 2: UV-Vis spectra of compounds **1**, **2** and **3,** followed by dissolution in the buffer solution (**a**) just after mixing and (**b**) after 3 days at 37 ^{o}C.

New Journal of Chemistry Accepted Manuscript

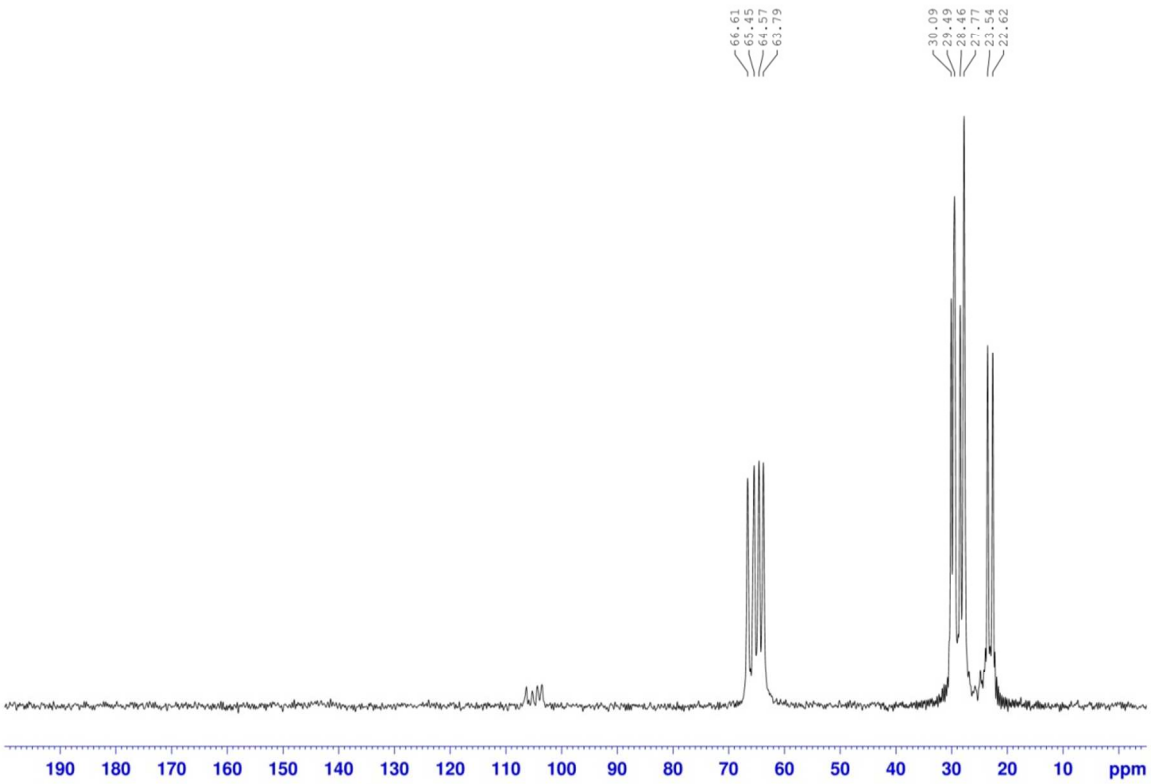

Figure 3: Solid state $^{13}C\{^{1}H\}$ NMR spectrum of complex **1.**

New Journal of Chemistry Accepted Manuscript

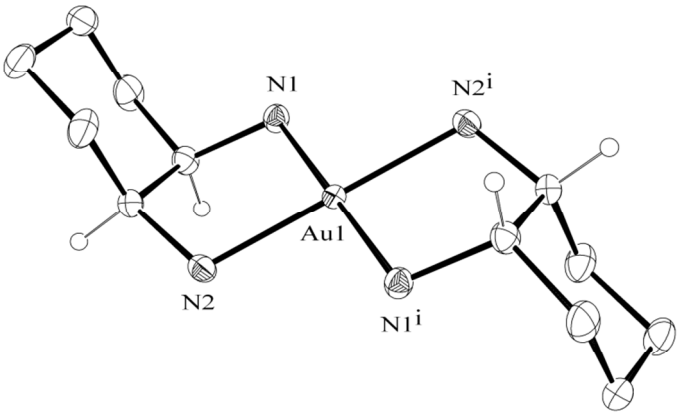

Figure 4: Molecular structure of compound **1.**

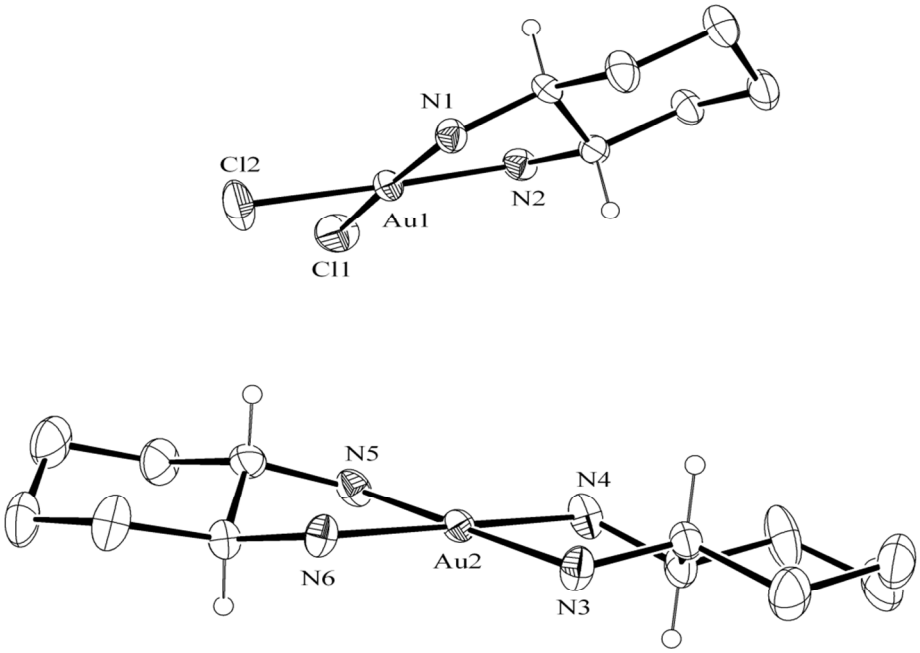

Figure 5 Molecular structures of the two components of co-crystal **2.**

New Journal of Chemistry Accepted Manuscript

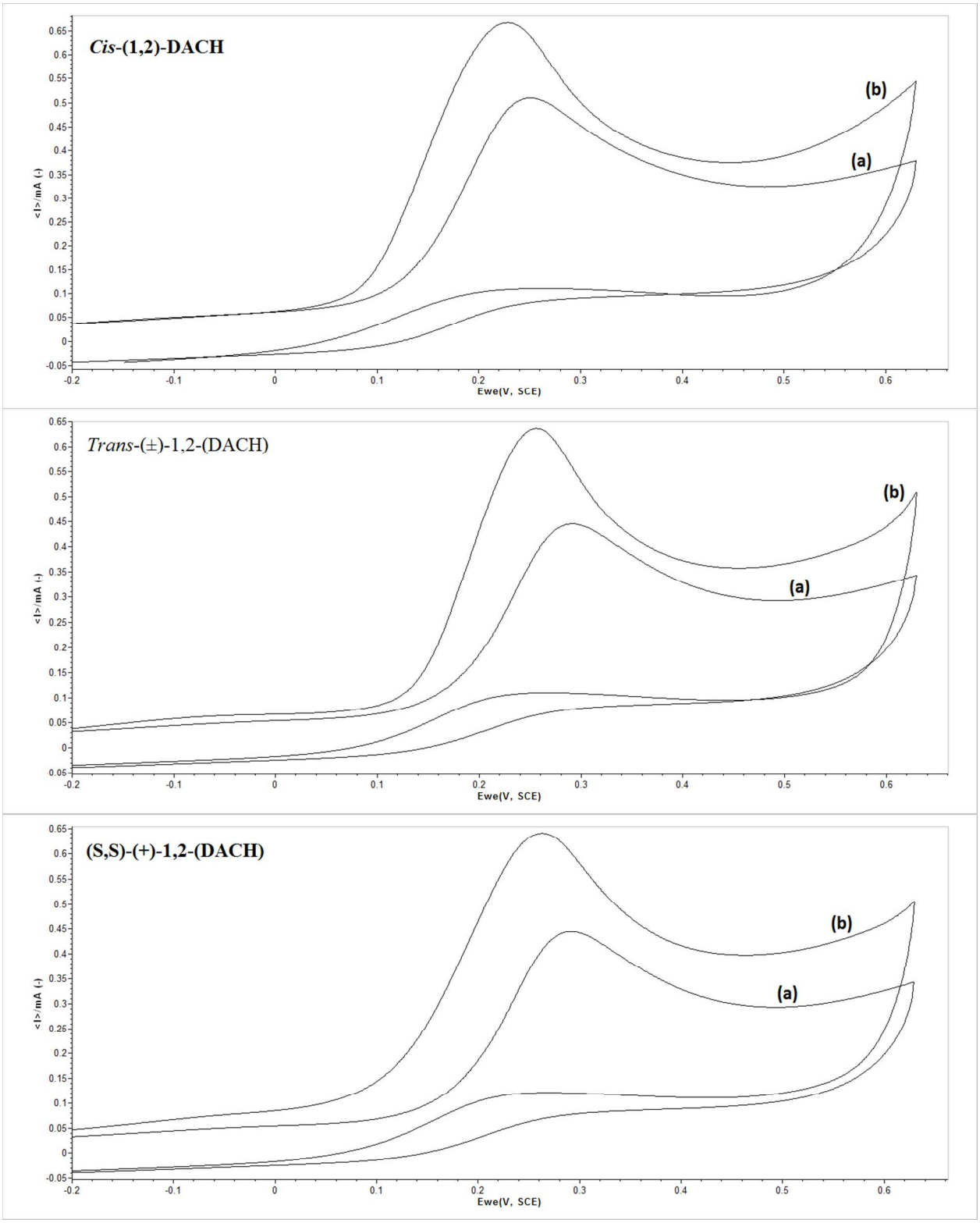

Figure 6. Cyclic voltammetric curves of the compounds **1, 2** and **3** and their corresponding mono-DACH gold(III) compounds. Curve labeled with (a) is corresponding to the bis-DACH, while, (b) corresponding to mono-DACH.

New Journal of Chemistry Accepted Manuscript